SANDIA REPORT
SAND2012-5496
Unlimited Release
July 2012

Cavity length dependence of mode beating in passively Q-switched Nd-solid state lasers

Nathan D. Zameroski, Michael Wanke, and David Bossert

Prepared by
Sandia National Laboratories
Albuquerque, New Mexico 87185 and Livermore, California 94550

Sandia National Laboratories is a multi-program laboratory managed and operated by Sandia Corporation, a wholly owned subsidiary of Lockheed Martin Corporation, for the U.S. Department of Energy's National Nuclear Security Administration under contract DE-AC04-94AL85000.

Issued by Sandia National Laboratories, operated for the United States Department of Energy by Sandia Corporation.

Available to DOE and DOE contractors from
U.S. Department of Energy
Office of Scientific and Technical Information
P.O. Box 62
Oak Ridge, TN 37831

Telephone: (865) 576-8401
Facsimile: (865) 576-5728
E-Mail: reports@adonis.osti.gov
Online ordering: http://www.osti.gov/bridge

Available to the public from
U.S. Department of Commerce
National Technical Information Service
5285 Port Royal Rd.
Springfield, VA 22161

Telephone: (800) 553-6847
Facsimile: (703) 605-6900
E-Mail: orders@ntis.fedworld.gov
Online order: http://www.ntis.gov/help/ordermethods.asp?loc=7-4-0#online

SAND2012-5496
Unlimited Release
July 2012

Cavity length dependence of mode beating in passively Q-switched Nd-solid state lasers

Nathan D. Zameroski, Michael Wanke, and David Bossert
Organization 2617 and 1118
Sandia National Laboratories
P.O. Box 5800
Albuquerque, New Mexico 87185-MSXXXX

Abstract

The beat frequencies, temporal intensity profile, and modulation depth of a flash lamp pumped passively Q-switched, Nd:Cr:GSGG monoblock laser with a Cr^{+4}:YAG Q-switch are investigated as a function of cavity length. The measured temporal widths are linearly correlated with cavity length and the modulation depths of the temporal waveforms are periodic in nature with cavity length, peaking at integer multiples of c/2nL. Simulations support measured trends in the pulse widths and beat frequencies as a function of cavity length.

ACKNOWLEDGMENTS

The authors would like to thank the following individuals who helped contribute to the experimental aspects of this work; Allen Gorby, Tony Coley, Art Fisher, Ed Barnet, and Paul Miller.

CONTENTS

FIGURES

NOMENCLATURE

YAG	Yttrium aluminum garnet
Nd	Neodymium
Cr	Chromium
GSGG	gadolinium scandium gallium garnet
SNL	Sandia National Laboratories
Cr^{+4}:YAG	Chromium doped YAG (this is the passive Q switch)
PSD	Power spectral density
FT	Fourier Transform
OC	output coupler
R	output coupler reflectivity
T_o	small signal transmission of Q-switch
HR	high reflection optical coating
AR	anti-reflection coating
L_C	physical cavity length
OPL	optical path length
OPL_M	optical path length master laser cavity
OPL_{EXT}	optical path length external cavity
QSML	Q switch mode locking

1. INTRODUCTION

The cavity length of a laser resonator plays an important role in determining the temporal intensity profile of the laser output pulse(s) in both passively Q-switched and passively Q-switch mode locked (QSML) solid state lasers [1-7]. Cavity length can influence pulse width and or repetition rate and determine whether a single, modulated, or burst of pulses underneath an envelope is generated. To achieve a single, smooth temporal pulse profile having a single rise and fall of the intensity rather than modulated or multiple pulse output, the difference in buildup time between any pair of longitudinal modes must be greater than the Q-switch pulse duration [2]. Short cavity lengths generally ensure this condition is met. Isyanova, et al. [2] derive analytic expressions for the temporal criteria, or difference in buildup time between longitudinal modes to achieve a single longitudinal mode laser pulse with no temporal instabilities.

In addition to the cavity length, the cavity output coupler reflectively (R) and the small signal transmission of the Q-switch (T_o) are the other resonator parameters that allow for optimization of pulse width for both passively Q-switched and passively QSML laser systems [8-11]. Passively Q-switched laser models developed by Patel et al. [8] and QSML models developed in [10,11] have built off the initial work of Degnan [9] and provide expressions to optimize Q-switch pulse energy and pulse width for a four level saturable absorber that has excited state absorption (ESA). The predicted pulse width of either of a single Q-switched laser pulse or the envelope of the QSML pulse train is linear with cavity length or round trip time (τ_{RT}), when T_o and R are held constant [8-11].

In this paper, the temporal width (full width half maximum), modulation depth, and beat frequencies of a flash lamp pumped, Nd:Cr:GSGG laser using a Cr^{+4}:YAG passive Q-switch are investigated as a function of cavity length. Cavity length regions are encountered where the pulse intensity profiles vary from little to no modulation to nearly a completely modulated waveform. The observed beat/mode locking frequencies at certain cavity lengths cannot be accounted for (explained) with current passively QSML laser models [10,11] in which the repetition rate of the QSML pulse train is τ_{RT}^{-1}. The observed beat/mode locking frequencies can however, be explained by coupled cavity mode-locking (CCML) affects [12,13] in which the

repetition rate or mode locking frequency can be a harmonic (integer multiple) of the fundamental mode locking frequency of the resonator. In these works [12,13] a two section resonator is purposely created by introducing a third mirror into the cavity, creating a 3 mirror Fabry-Perot resonator. The reflectivity of the 3rd mirror used in these previous publications [12,13] are an unknown anti-reflection (AR) coating and 20 %. We find/show that coupled cavity effects are just as pronounced due to the $< 10^{-3}$ anti-reflection (AR) coating on the output side of the laser rod.

This paper is organized as follows. Section II discusses the experiment and presents experimental data. In the section III, a theoretical model initially developed by Coldren [14] for a two section coupled cavity laser is expanded upon to include gain roll off of the lasing transition and used to interpret the experimentally measured beat frequencies. Section III also discusses the temporal criteria described in [2] for our laser cavity as a function of pump rate and gain roll off versus cavity length. Previous work by Isyanova et al [2] investigated the temporal criteria, difference in buildup time between longitudinal modes τ_d, for fixed cavity lengths and pump rates but varying values T_o. We numerically determine τ_d for our cavity for fixed values of R and T_o but varying cavity length and pump rate. The difference in buildup time between longitudinal modes is compared to simulated and experimentally measured pulse durations to see if the conditions to achieve smooth pulses are satisfied. We show that in flash lamp pumped systems the difference in buildup time between longitudinal modes is largely dependent on the pump rate. For rapid time to fire applications, this pumping rate may limit the ability to achieve temporally smooth pulses in passively Q-switched laser systems.

2. EXPERIMENT

2.1 Experimental description

Figure 1 shows a schematic of the laser cavity. The host crystal is gadolinium scandium gallium garnet (GSGG) and is doped with Neodymium (Nd) and Chromium (Cr). The Nd^{+3} and Cr^{+3} doping concentrations are ~ $2x10^{20}$ cm^{-3} and ~ $1x10^{20}$ cm^{-3} respectively. The spectroscopic properties of Nd:Cr:GSGG can be found in references [15,16]. The gain media is 4.5 cm in length, and except for a 3 mm wide flat surface running the length of the gain rod was circular in cross section with a radius of 3 mm. One end of the rod has a high reflection (HR) coating with reflectivity > 0.99 and other end has an anti-reflection (AR) coating with measured reflectivity of ~ $4x10^{-3}$ at 1061 nm (the lasing wavelength). The cavity output coupler (OC) optic and the high reflectivity end of the gain rod are flat mirrors and create a quasi-stable resonator. The reflectivity of the OC is 0.6. The distance between the Q-switch and output coupler was kept between 3 and 4 mm throughout experiments. The gain rod was side pumped by a single 45 mm long Xenon flash lamp (450 Torr). To distribute the pump light throughout the gain rod, the flash lamp light was directed into the gain rod using a diffuse, barium sulfate coated, double-parabolic reflector. The flash lamp was driven by a ~ 40 μs (FWHM) current pulse. The laser was fired at a rate of 0.016 Hz for all data acquisition.

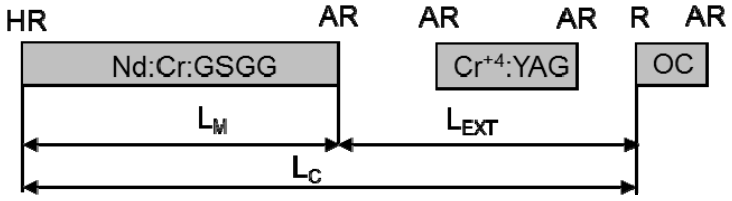

Figure 1. Schematic of laser cavity L_M = master cavity physical length = 45mm, L_{EXT} = external cavity length, L_C = physical cavity length. HR= high reflector coating, AR= anti-reflection coating, R= output coupler coating with reflectivity R = 0.6. The index of refraction of Nd:Cr:GSGG and Cr^{+4}:YAG are 1.949 and 1.82 respectively. It is noted here, that although the gain rod with AR coating is designated as the master cavity, it cannot lase off of the AR coating surface.

Cr^{+4}:YAG with a small signal transmission of 0.35 was used as the passive Q-switch. The cross section and length of the Q-switch are ~ 6 mm x 6 mm x 5 mm. The Q-switch was AR coated on both surfaces at 1061 nm with a reflectivity of ~10^{-3}. The spectroscopic properties and saturation dynamics of Cr^{+4}:YAG can be found in [17,18]. Because of its four level structure and

drastically different excited state lifetimes (1^{st} excited lifetime ~ 3.5 μs [19] and 2^{nd} excited lifetime of ~ 100 ps to 550 ps [20,21]) Cr^{+4}:YAG has been used to obtain temporally smooth Q-switched pulses [22,23] and also QSML pulse trains [24].

2.2 Data collection and analysis

The measured Q-switch pulse energy was found to be relatively independent of cavity length. For approximately 330 temporal waveforms collected as a function of cavity length, the measured pulse energy was 127 ± 11 mJ. The laser was multimode. The predicted laser energy using Equation (8) of Patel [8], assuming a single pass transmission of 0.98, is 156 mJ to 192 mJ depending on the assumed ratio of the ground state (σ_{gs}) to excited state (σ_{es}) absorption cross sections of the Q-switch. For these calculated energies, the ratios are 3.6 and 4.9, respectively [18]. The measured results are ~ 19 % to 34 % smaller than what is predicted by the model. One possible explanation for this discrepancy is that the model assumes that the entire laser rod area is uniformly pumped and contributes to lasing, whereas measured near field images of the laser output indicated non-uniform pumping in the rod such that some parts of the rod did not contribute to lasing. Diffraction losses should also decrease the output energy, especially as resonator length increases, but are not accounted for in the model.

Temporal waveforms were acquired with a photomultiplier tube with a ~90 ps rise time and ~ 90 ps fall time connected to a 20 GHz oscilloscope. The measured 3dB bandwidth of the measurement systems is 3.4 GHz. **Figure 2** shows a temporal waveform of the intensity of a single Q-switched laser pulse and its corresponding Fourier Transform (FT) for a physical cavity length L_C = 310 mm. There is significant mode beating present at 1680 MHz. The 1680 MHz beat is the 4^{th} harmonic of the fundamental mode spacing of $c/[2(n_M L_M + n_{air} L_{air} + n_Q L_Q)]$ = 420 MHz. Here L_M, L_{air}, and L_Q are the physical lengths of the gain rod, the air gaps in the cavity, and the Q-switch. n_M, n_{air}, and n_Q are the index of refraction the gain rod, air, and the Q-switch. The fundamental is discernible near the peak of the pulse, appearing as a periodic (high-high-low-low) fluctuation of the individual peaks that repeats every 4 peaks.

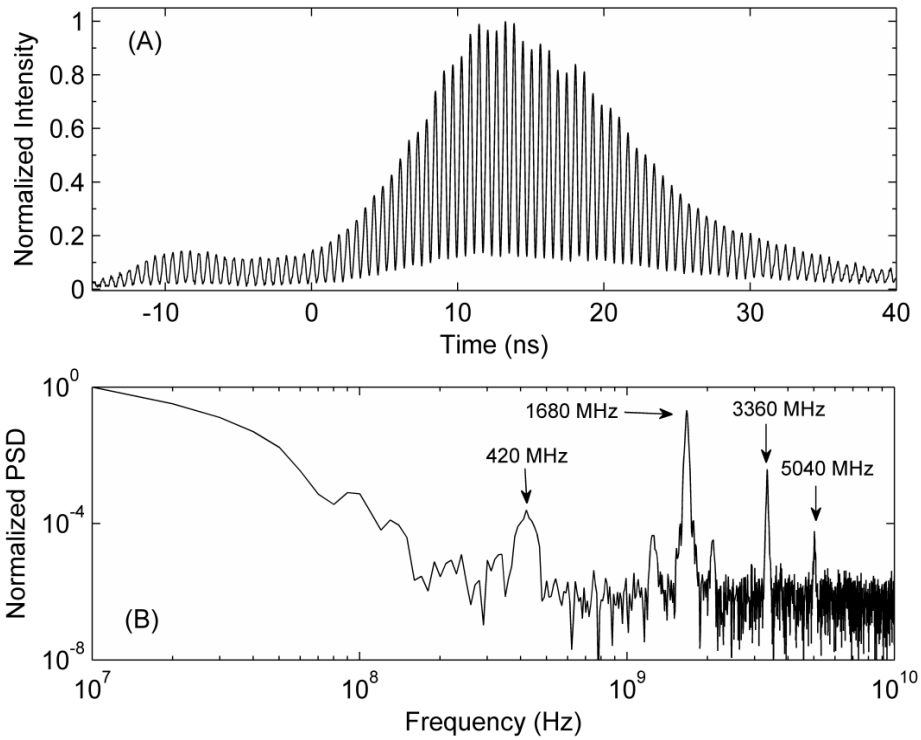

Figure 2. (A)-Temporal waveform of a single shot for L_C= 310 mm. Pulse envelope FWHM is 16 ns. Modulation depth = 0.9. Modulation depth is defined as 1- (Valley value / Peak value) and is bounded between zero and one. A value of zero indicates a smooth pulse while a value of one indicates a completely modulated pulse. The peak value in the pulse profile is where the intensity is maximum. The valley value in the pulse profile is where the intensity is minimum and located nearest to the peak value. (B)- Normalized power spectral density (PSD) Fourier Transform. The free spectral range (FSR) of this cavity length (L_C) is 420 MHz. The side bands of the 1680 MHz beat are at 1260 and 2100MHz.

The modulation depths and beat frequencies extracted from the measured temporal intensity waveforms are shown versus cavity length in **Figure 3 A&B.** The modulation depth is the largest when $\varepsilon = OPL_{EXT}/OPL_M$ is close to 1, 2, 3, and 4. OPL_M is the optical path length of the laser rod, designated as the master cavity, and OPL_{EXT} is the optical path length of external cavity formed by the AR coating on the gain rod and the output coupler optic and includes the Q-switch optical path length and air gaps. As shown in **Figure 2**, multiple beat frequencies between axial modes can occur at a given cavity length. We see that the largest amplitude in the PSD spectrum occurs at the harmonic of the FSR closest to 1700 ± 70 MHz, when ε is near integer values. This frequency corresponds to the free spectral range (FSR_M) of 1709 MHz calculated for a 45 mm long laser rod with an index of refraction of 1.949. Thus even though the laser rod has an anti-reflection coating on it, there appears to be enough residual reflection to result in a coupled cavity. Harmonic mode locking is predicted to occur when the ε = n/m [13] for integer values of

n and m. When ε = 1, 2, 3, 4…, the predicted dominate mode locking frequency is 1709 MHz and when ε = n/2, where n= 1, 3, 5, 7…, the predicted mode locking frequency is $2FSR_M$.

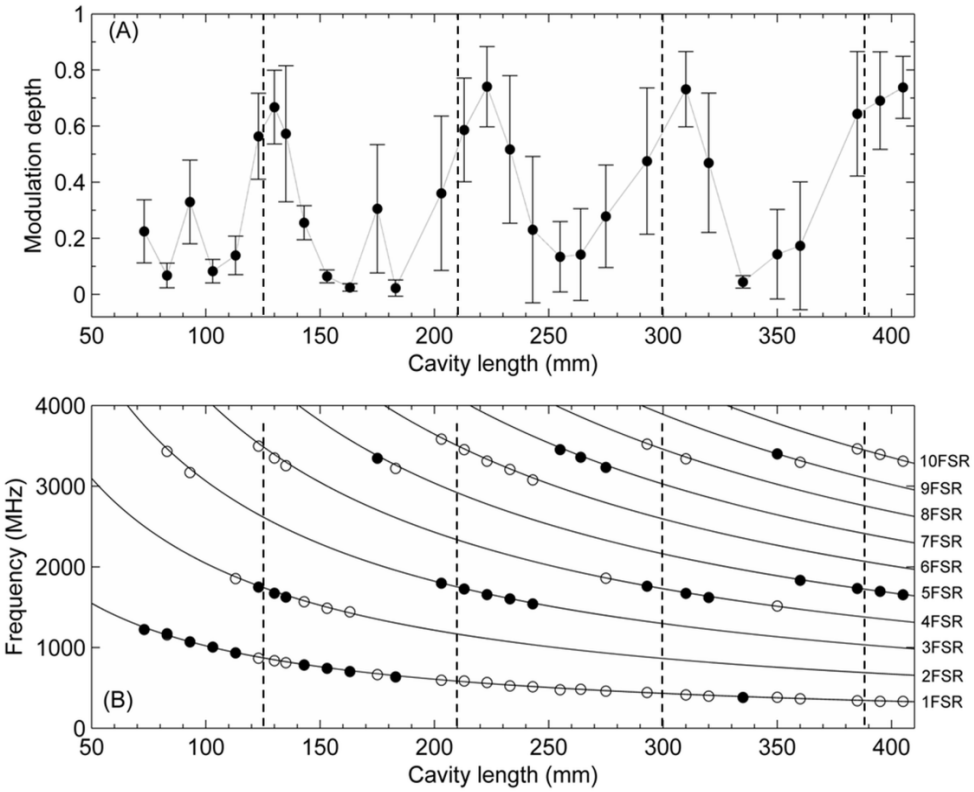

Figure 3. (A)- Modulation depth versus cavity length. The experimental data points are the average of approximately eleven recorded waveforms and the error bars are the standard deviation for the set of measurements at each cavity length. (B)-Beat frequencies vs. cavity length. Solid lines are simulated integer multiples of FSR of L_C from 1FSR to 10FSR, ○ = frequencies present in the FT, ● = strongest beat frequency in the FT. Vertical dashed lines correspond to ε =1, 2, 3, 4 and cavity lengths of 124, 211, 300 and 389 mm, respectively. ε is a linear function of L_C and for our cavity this relationship is: $\varepsilon(L_C) = (0.0114/\text{mm})L_C - 0.409$.

At cavity lengths of 83, 103, 153, 163, 183, and 335 mm pulses with low modulation depths are measured on nearly every laser shot and the strongest beat is at the FSR of the overall (physical) cavity length (L_C). At these lengths ε has values near (1/2), (3/4), (4/3), (3/2), (5/3), and (17/5). These fraction values correspond to mode locking frequencies of 3418, 6836, 5127, 3418, 5127, and 8545 MHz, respectively. It is possible that there was significant modulation depth and longitudinal mode beating at these cavity lengths, but that the modulation frequency was higher than the detection bandwidth resulting in instrumentally smoothed pulses with small modulation depths. **Figure 4** shows the calculated dominate beat/mode-locking frequencies as a function of ε

= n/m for integer values n and m. The beat frequency is given by m*FSR_M. Going to even larger values of m should increase the beat frequency. However, there is a limit to the allowed mode locking frequency or repetition rate in a QSML pulse train. The gain or lasing bandwidth limits the maximum mode locking frequency by controlling the number of longitudinal modes that can reach threshold and thus beat together in phase, a required condition for mode locking [25]. Another mechanism that limits the mode locking frequency is the excited state lifetime of the Cr^{+4}:YAG Q-switch. This transition must be able to modulate the gain/loss of the resonator on a time scale faster than the cavity round trip time to phase lock longitudinal modes [25]. Using the published excited state lifetime values in the literature of ~ 550 to 100 ps, the mode locking frequency (repetition rate) is estimated to be from 1.8 GHz to 10 GHz.

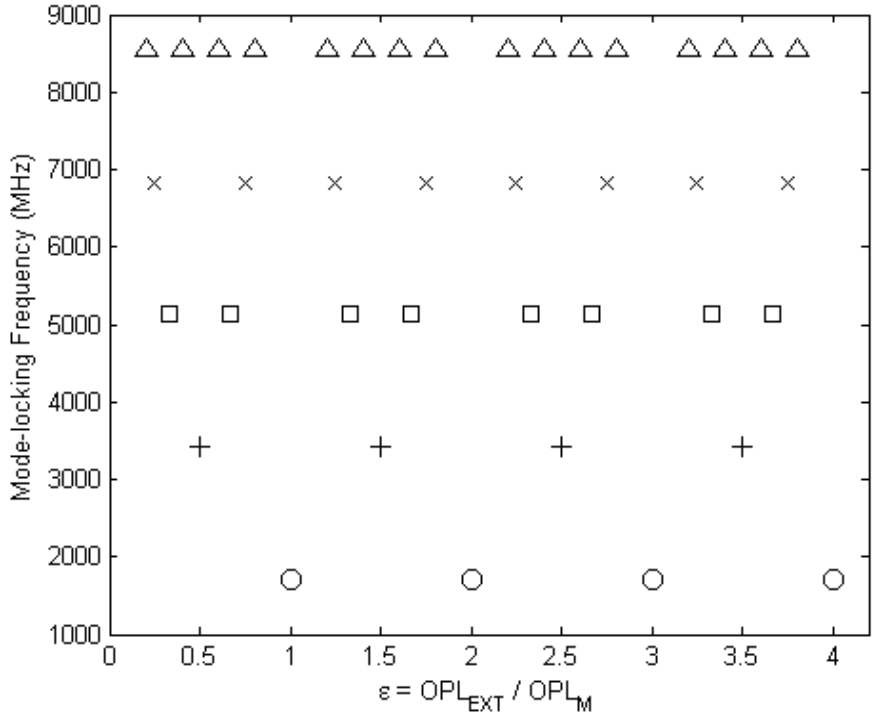

Figure 4. Predicted dominate harmonic mode locking frequency versus ε. O for ε = integer multiples of 1, + for ε = odd integer multiples of (1/2), □ for ε = integer multiples of (1/3), × for ε = integer multiples = (1/4), and Δ for ε = integer multiples of (1/5).

At ε = n/2, for n = 3, 5, and 7, (cavity lengths ~ 175 mm, 260 mm, and 350 mm) the strongest measured beat frequency occurs at ~2FSR$_M$ but the modulation depth is smaller and the variation in modulation depth, intensity profile, and beat frequency strengths between shots is greater than when ε equals an integer value. **Figure 5** shows two consecutive laser shots at L_C = 175 mm (ε ~ 3/2). **Figure 5B** shows the FT of the temporal waveform in **Figure 5A**. The strongest beat frequency occurs at 3340 MHZ (~2FSR$_M$ or 5FSR of L_C) and the highest frequency component that is resolvable is 6680 MHz. **Figure 5 C** shows the temporal waveform following the laser shot present in **Figure 5 A.**

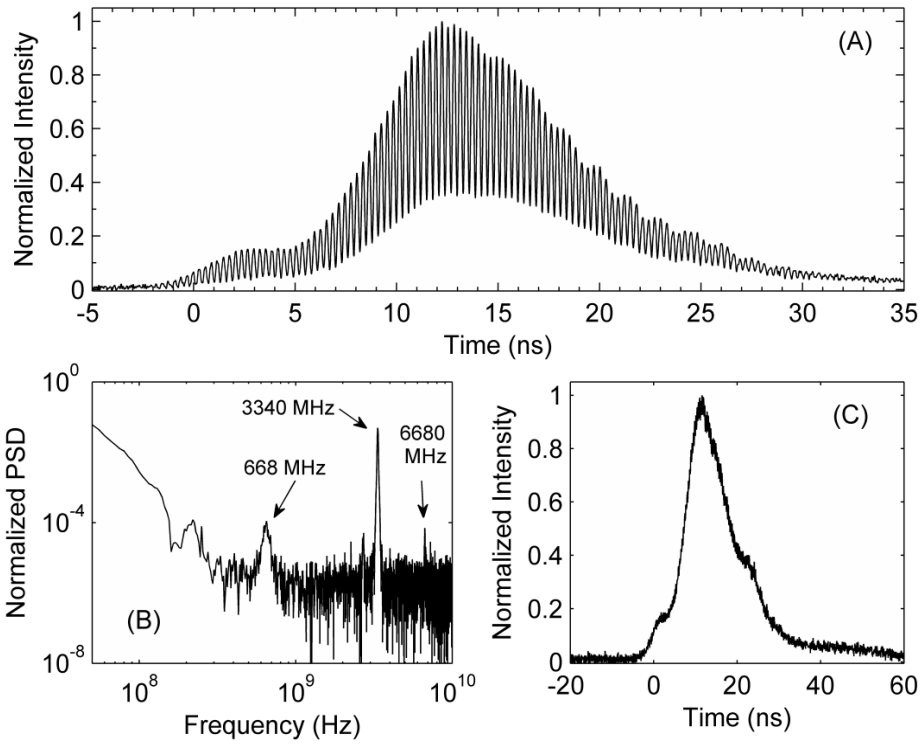

Figure 5. (A)-Temporal waveform intensity of single Q-switched laser pulse at L_C= 175 mm. Modulation depth ~ 0.7 and pulse width ~ 10 ns. (B) Fourier Transform of the temporal waveform in (A) show strongest beat at 3340 MHz. (C) Temporal waveform intensity of single Q-switched laser pulse following shot after (A). Modulation depth ~ 0.1 and pulse width ~ 11 ns.

3. DISCUSSION

3.1 Mode beating dynamics

Since the mode beating dynamics depends on which axial modes are lasing, we need to determine which modes are excited and how the coupled cavities influence these modes. The modes that are excited will depend on the threshold for each mode. To determine the threshold gain differences between the longitudinal modes of the overall laser cavity, a below-threshold analysis was implemented, following Coldren's [14] work (not repeated here) modeling the behavior of coupled-cavity semiconductor lasers. In our case, however, the two coupled cavities of the laser consist of the laser rod as one cavity and the propagation (OPL_{EX}) between the rod output coupler optic as the other cavity. The residual 10^{-3} reflectivity of the AR coating end of the rod serves as the dividing wall between the two cavities. The wavelengths and threshold gains of the laser modes can be determined by solving for the poles of the linear transfer function, H(ν), Equation (4) [14], describing the composite resonator.

$$H(\nu) = \frac{t_1 t_2 S_{21} e^{-ik_1 l_1} e^{-ik_2 l_2}}{1 - D(\nu)} \tag{1}$$

Where

$$D(\nu) = (S_{12}S_{21} - S_{11}S_{22}) r_1 r_2 e^{-2ik_1 l_1} e^{-2ik_2 l_2} - r_1 S_{11} e^{-2ik_1 l_1} - r_2 S_{22} e^{-2ik_2 l_2}. \tag{2}$$

The S_{ij} represent scattering coefficients describing the antireflective facet coating on the laser rod. r_1, r_2 (t_1,t_2) are amplitude reflection (transmission) coefficients for the resonator end mirrors, while k_1, k_2 are complex propagation constants within the two sections of the resonator of length l_1 and l_2.

Figure 6a diplays one minus the denominator of *H* versus frequency for a resonator with rod length of 45 mm (OPL_M=87.7mm) and an external optical path length OPL_{EXT} = 87.7mm thus ε = 1. The corresponding physica cavity length (L_C) is 124 mm. For the following calculations, we model a single layer AR coating with power reflectivity of $1x10^{-4}$ and an outcoupler reflectivity of 0.6. Dots indicate the allowed longitudinal mode frequencies, which are roots of the denominator of *H*. The associated threshold gains for those frequencies are given in **Figure 6b**). It is clear that adacent modes (nearest neighbor in frequency) have a significantly increased

threshold gain. The threshold gain of the lower threshold set of modes, separated by two free spectral ranges (every other mode), is unaffected by coupled-cavity effects, varying only slightly due to gain rolloff from the lasing line shape. This behavior is consistent with the experimental observations, and a beat frequency of (ε + 1)FSR of the overall cavity length is always obtained where the optical cavity length ratio of the two cavity sections is an integer. See for example, **Figure 3** when ε is an integer value the strongest beat occurs at (ε + 1)FSR. At cavity lengths near 124 mm (ε ~1), the strongest beat observed occurs at 2FSR of L_C, i.e. every other mode is beating together.

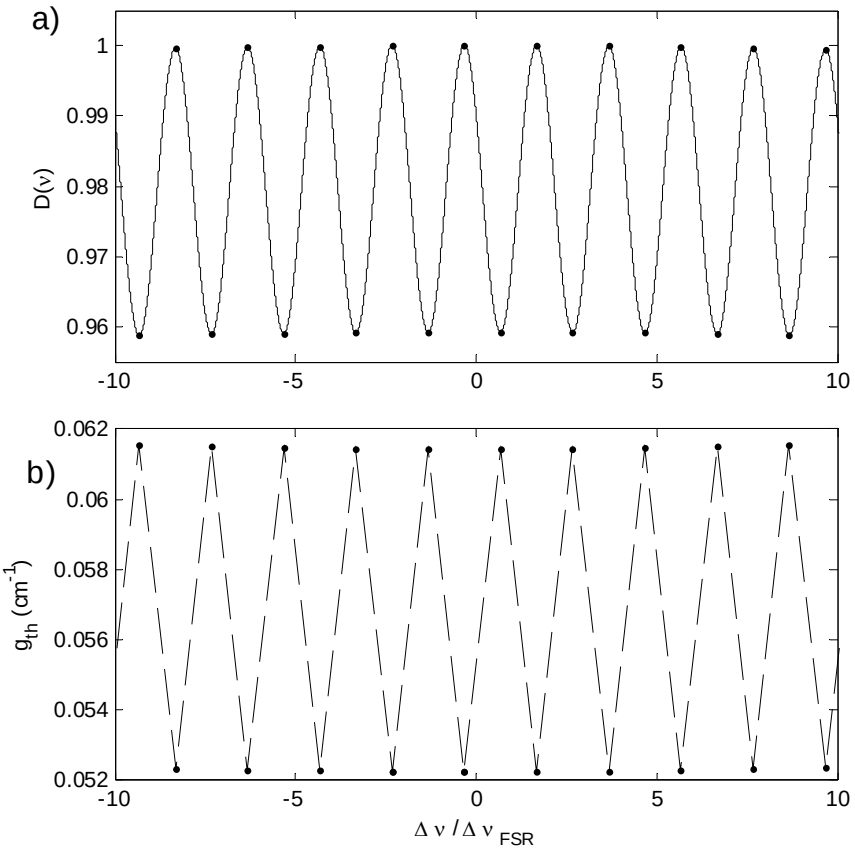

Figure 6. a) One minus the denominator of the transfer function for L_C=124 mm. b) Threshold gain coefficient of the allowed longitudinal modes, indicated by dots.

Where this condition is not satisfied (ε ≠ interger value), the mode structure is more complicated. As an example, **Figure 7** shows the case where OPL_{EXT} is 1.5 times the optical length of the rod (ε= 3/2). The calculated cavity length for this simulated condition is 168 mm. Here, the set of low threshold gain modes, unaffected by the presence of a coupled-cavity, are located at five

times the free spectral range of the laser cavity. This was the case experimentally as seen **Figure 5A** . Experimental data at L_C = 175 mm shows that the strongest beat is obtained at 3340 MHZ and is 5FSR of L_C.

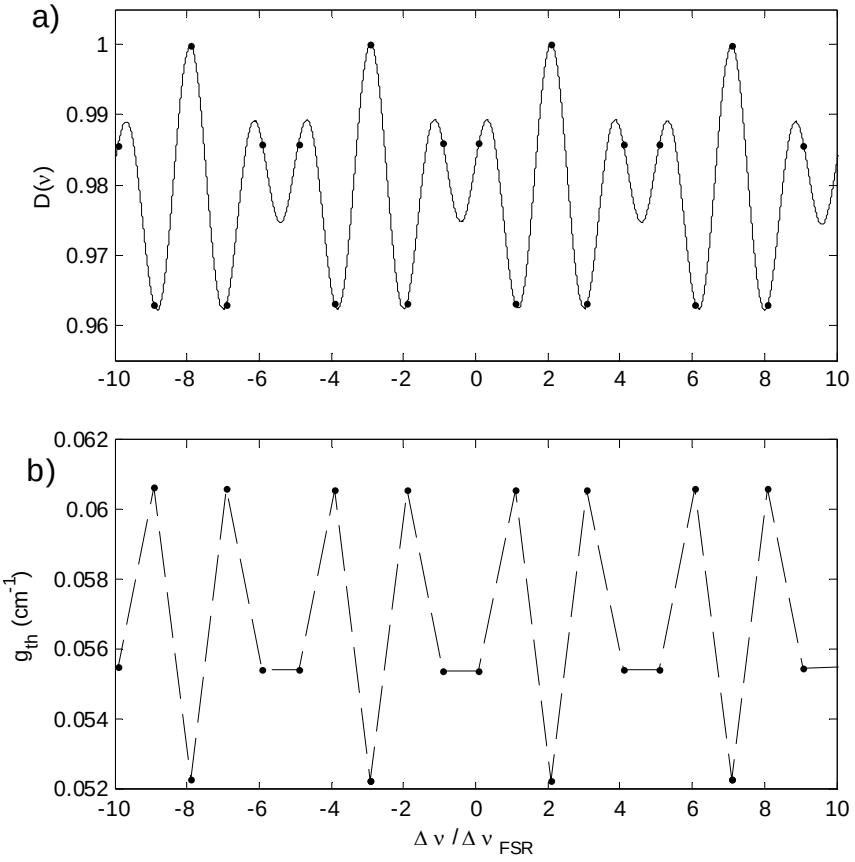

Figure 7. One minus the denominator of the transfer function for a 167 mm long resonator. b) Threshold gain coefficient of the allowed longitudinal modes, indicated by dots.

The above simulations were carried out for a specific optical path length of the external cavity. There are, however, potentially sizeable effects from small length variations on the order of a wavelength, that "piston" the relative phase of the two cavity sections. **Figure 8** shows the piston dependence of the threshold gain for the same two cavity lengths given above. In **Figure 8a** (L_C =124 mm, ε = 1) and **Figure 8b** (L_C =168 mm, ε = 3/2), the solid (green curve) and dashed lines (red curve) correspond to the gain difference (Δg_{th}) between the lowest threshold mode and the next two competing modes. One can see that while there are minor variations with respect to length piston, the threshold gain differences between the first three modes (modes with lowest thresholds) are relatively flat and on the order of the gain rolloff (~ 10^{-5} to10^{-4} cm^{-1}).

On the other hand, as indicated by the dash-dotted lines (black) in **Figure 8a &b**, the gain difference between the lowest threshold mode and its nearest neighbor in frequency are much larger and are a periodic function of frequency. (**Note** that these traces are divided by 20 for comparison purposes.) The modal discrimination between the lowest and highest threshold gain modes is directly proportional to the amplitude reflectivity of the AR coating, which is given by the magnitudes of the scattering parameters and . We expect these modes to be heavily rejected by the overall resonator, even for very small reflectivity from the AR coating.

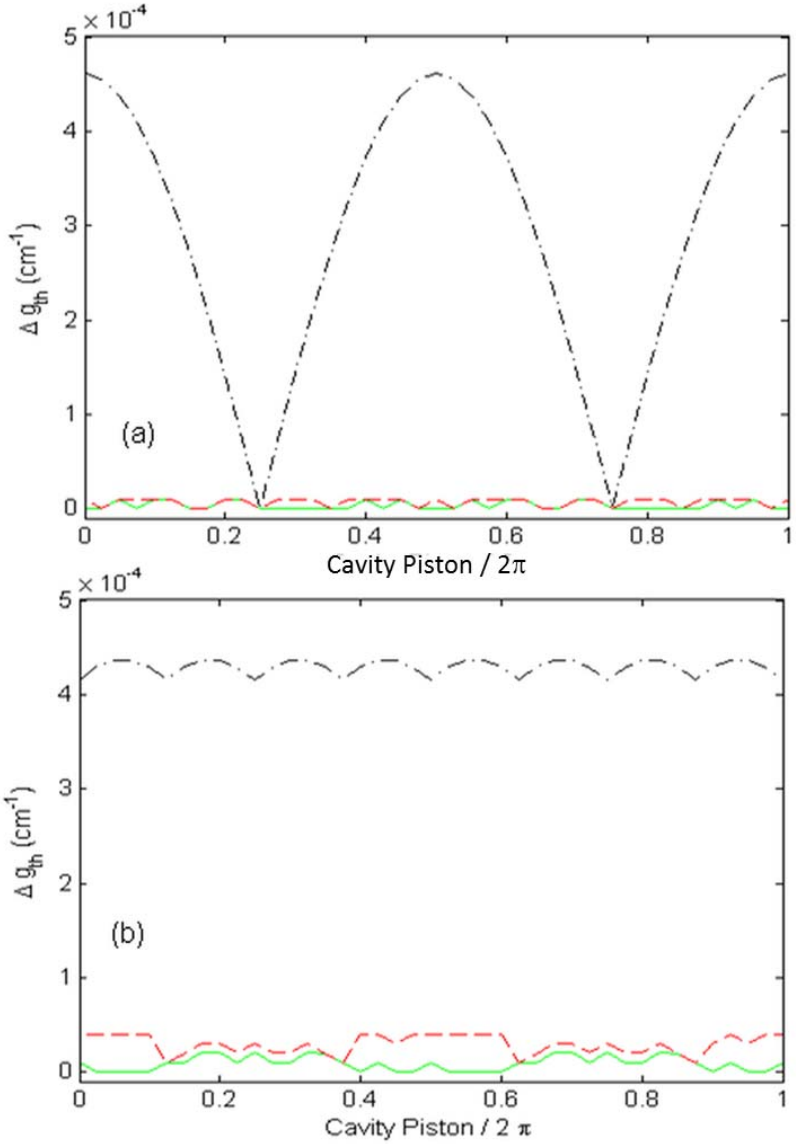

Figure 8. Threshold gain versus cavity length piston for a) L_C=124mm and b) L_C=168mm. Dot-dashed (black) curves are divided by 20 for comparison.

3.2 Pulse widths (simulated & experiment) and temporal criterion

Figure 9 shows the measured pulse widths (FWHM) versus cavity length. Theory [8] predicts that pulse width is linear with L_C with a slope of 0.027 ns/mm with a y-intercept of 1.47 ns for our cavity. A linear least squares fit of the experimental data yielded a slope of 0.04 ± 0.001 ns/mm with a y-intercept of 3.3 ± 0.2 ns. The linear correlation coefficient R and P-value of the linear fit are 0.85 and << 0.001, respectively. The large pulse widths for L_C > 350 mm are due to etalon effects which have also been observed by Becker [26] for harmonic mode locking in a Nd:YAG laser.

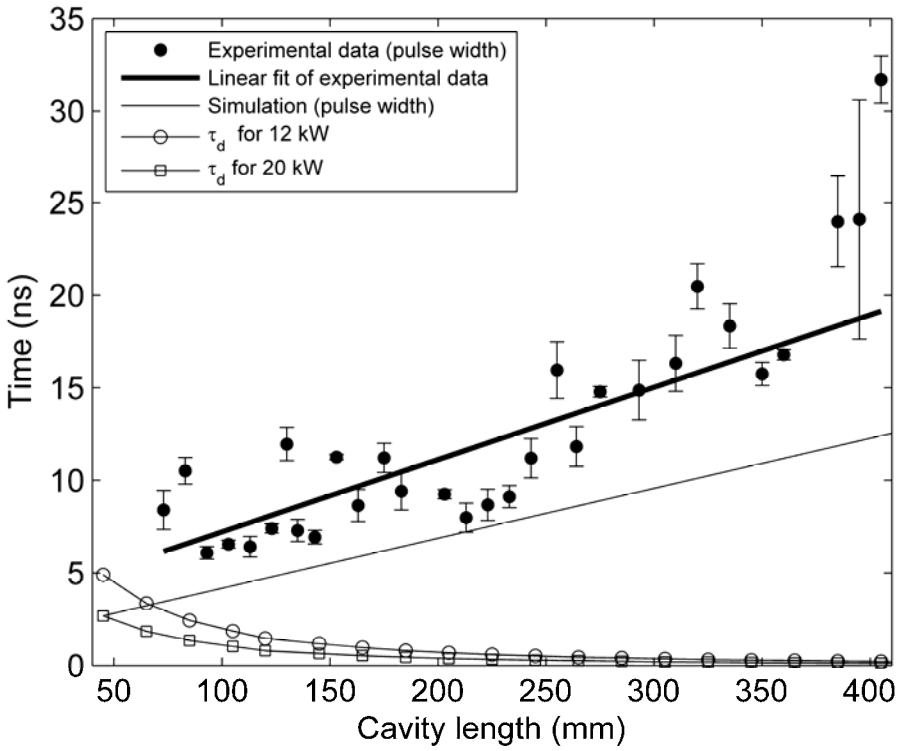

Figure 9. Q-switched pulse width and difference in buildup time (τ_d) verses cavity length. Error bars on the pulse widths are the standard deviation for the set of measurements at each cavity length.

The simulated pulse width curve is roughly 3 to 5 ns smaller than the linear fit of experimental data. In the model [8], for fixed values of R, T_o, and cavity length, the pulse width is controlled by the simulated emission cross section and the ratio of the ground state to the excited state absorption cross sections of the Q-switch. When floating the ratio (σ_{gs}/σ_{es}) in the model within the published ranges (3.6 to 4.9) [18], the y-intercept of theoretical curve can at most be increased by 800 ps and the slope changes slightly. Therefore, the uncertainty in the ration cannot explain the discrepancy between the predicted (simulated) and measure results. On the

other hand, the spatially inhomogeneity of gain which resulted from non-uniform pumping could possibly explain the larger pulse widths measured in the laboratory. The rod is pumped more towards the flash lamp side and hence will have higher gain. The beam will take some time to walk (diffract) out from this point when lasing started to other sections of the rod when gain exists. A thorough discussion of spatial diffractive filling of a passively Q-switch Nd:YAG laser with Cr^{+4}:YAG passive Q switch is given by Zabkar [27].

The simulated pulse width curve is determined numerically by solving the rate equations in Patel [8] instead of using the analytic approximation for pulse width in [4], i.e. Eq. A.1. The simulated pulse width is slightly dependent of pump rate. It is noted here that numerical solutions of the rate equations in [8] produce Gaussian shaped pulse and the pulse widths are ~ 6 % larger than the pulse widths obtained by using the pulse width approximation in [8], (i.e. Eqn. A.1.) which assumes an triangle for the pulse shape.

Figure 9 also shows the simulated difference in buildup time (τ_d) between longitudinal modes as a function of cavity length for pump powers of 12 kW and 20 kW with corresponding pump rates of 3.84×10^{22} $s^{-1}cm^{-3}$ and 6.4×10^{22} $s^{-1}cm^{-3}$. The difference in buildup time is a function of cavity length, gain roll off (assumed Lorentzian lineshape with FWHM of 345 GHz and peak emission cross section $=1.59 \times 10^{-19}$ cm^2), and pump rate for constant values of R and T_o. τ_d is determined numerically by solving the rate equations in [4] instead of using the approximation (Eqn. (8)) of reference [2]. τ_d is determined in the simulations by measuring the difference in time between the center location of one pulse to center location the next pulse as a function of cavity length. As cavity length increases, gain roll between longitudinal modes decreases and τ_d between longitudinal modes decreases.

The pump rate of 12kW is based off the difference in time between the laser emission monitored by a photodiode and the rising edge (slope/edge) of the light emission of the flash lamp. This time difference was measured between 45-55 μs for nearly all laser shots in the laboratory. This time was controlled by the initial charge voltage on the capacitor in the pulse generating circuitry. Observe in **Figure 9**, as the pump rate/power increases, τ_d decreases. For the 12kW pump, the simulated pulse width and τ_d curves cross at a cavity length of ~ 65 mm and at 20 kW

this cross over is at ~ 45 mm. Based on the temporal criteria along [2], smooth pulses should occur for cavity lengths < 65mm and < 45 mm for pump powers of 12 and 20 kW respectively. According to [2] mode beating or modulated temporal intensity waveforms will occur for cavity lengths > 45 mm and > 65 mm for pump power of 12 and 20 kW.

From **Figure 9** and **Figure 3** we give a few possible explanations for the lack of beat frequencies and low modulation depths at cavity lengths < 103 mm; 1.) The temporal criterion for smooth pulses is achieved or 2.) the excited state lifetime of the Q-switch is approaching the cavity round trip time and hence the absorber cannot recover fast enough for the next circulating pulse in the resonator . At cavity lengths beyond the cross over point of the simulated pulse width and τ_d curves in **Figure 9**, modulated temporal intensity waveforms should always be observed according to the temporal criteria [2], however this is not the case for cavity lengths of 153 mm, 163 mm, 183 mm, and 335 mm where the modulation depths are small, < 0.1 and the strongest beat occurs at FSR of L_C. For both the short cavity lengths (< 103 mm) and longer cavity lengths (>103 mm) the mode beating /mode locking frequency is likely beyond the detector resolution and the waveforms are smoothed from instrument response. A faster detector would allow confirmation of the lack the of higher beat frequencies at cavity lengths where coupled cavity mode locking effects are expected to increase the repetition rate of the QSML pulse train.

Future work would involve using a faster detector and measuring the temporal intensity waveforms at cavity lengths where the mode locking frequency is expected to be $m*FSR_M$. The exited state lifetime of the Cr^{+4}:YAG passive Q switch could be indirectly inferred from the measured mode locking frequency of the QSML pulse train.

4. **CONCLUSION**

This manuscript has investigated the beat frequencies, modulation depths, and temporal intensity profiles of a flash lamp pumped passively Q-switched neodymium laser as a function of cavity length. The measured temporal widths were linearly correlated with cavity length and are generally 3-5 ns longer than simulated pulse widths. The modulation depths of the temporal waveforms were measured to be periodic in nature with cavity length, peaking at integer multiples c/2nL. The measured beat frequencies were explained by implementing a below-threshold coupled cavity laser model following previous published work. Existing passively QSML laser models should be modified to include the effects of coupled cavities to capture the increased repetition rates and mode locking frequencies observed in experimental data.

The difference in build-up time between longitudinal modes was numerically investigated for different pump powers as a function of cavity length and included gain roll off. Simulated results indicate that mode beating will always occur in our cavity for the pump rates >12 kW for cavity lengths > 65mm. Large or fast pumping rates lead to a decrease or shorting in the difference in buildup time between longitudinal modes. The pumping rates used in the experiments may be a limiting factor in achieving temporally smooth, single longitudinal mode pulses in flash lamp pump passively Q-switch solid state lasers. For rapid time to fire applications, cavity length, AR coating reflectivity, cavity design (implementation of Brewster windows to reflection light out of the resonator), and pumping rate must all be considered, if a smooth temporal intensity waveform is required from a passively Q-switched solid state laser.

5. REFERENCES

1. J.J. Zayhowski " Passively *Q*-switched Nd:YAG microchip lasers and applications", Journal of Alloys and Compounds 303–304 pg. 393-400 (2000)

2. Y. Isyanova and D.Welford, "Temporal criterion for single frequency operation of passively Q-switched lasers", Optics Letters Vol.24. 15, pg 1035-1037.(1999)

3. A.J. DeMaria, D.A. Stetser and H.Heynau, "Self-mode-locking of lasers with saturable absorbers" Applied Physics Letters Vol. 8, No.7, 174-176 (1966)

4. E.G. Lariontsev and V.N. Serkin, "Influence of resonator length on the dynamics of generation of ultrashort light pulses", Sov. J. Quant. Electron, Vol. 4, No. 10 pg. 1204-1207 (1975)

5. E.L. Klochan, L.S. Kornieko, N.V. Kravtsov, E.G. Lariontsev, and N.I. Naumkin, " Some characteristics of a laser with a delay line and a passive Q switch", ", Sov. J. Quant. Electron, Vol. 3, No. 5 pg. 392-394 (1974)

6. N.V. Kravtsov, and Y. P. Yatsenko, "Effect of resonator length on laser output with passive mode locking" Sov. Phys. Tech. Phys. Vol. 22, No. 11, pg. 1409-1410 (1977)

7. R.E. McClure, " Mode locking behavior of a gas laser in long cavities", Applied Physics Letters, Vol. 7, No. 6, pg.148-150 (1965)

8. F.D. Patel and R.J. Beach, "New Formalism for the Analysis of Passively Q-Switched Laser Systems" IEEE J. QE. Vol. 37, No. 5, 707-715 (2001)

9. J.J. Degnan, "Theory of the Optimally Coupled Q-Switched Laser", IEEE.J.QE. Vol. 25. No. 2, 214-220 (1989)

10. J. Zhao, S. Zhao, K.L Fanmin, G.Zhang, "Optimization of passively Q-switched and mode-locked lasers with Cr+4:YAG saturable absorber", Optics Communications Vol. 284, 1648-1651, (2011)

11. Y.F Chen, J.L. Lee, H.D. Hsieh, and S.W.Tsai, "Analysis of Passively Q Switched Lasers with Simultaneous Mode locking", IEEE.J.QE, Vol 38.No.3, 312-316 (2002)

12. J. Hirano and T.Kimura, "Multiple mode locking of lasers", IEEE J. QE. Vol. QE-5, No. 5, 219-225 (1969)

13. G.S. He, Y. Cui, G.C. Xu and P.N. Prasad, "Multiple mode-locking of Q-switched Nd:YAG laser with a coupled resonant cavity", Optics Communications 69, 321-329, (1993)

14. L.A. Coldren and T.L. Koch, "Analysis and Design of Coupled –Cavity Lasers –Part 1: Threshold Gain Analysis and Design Guidelines", IEEE.J.QE. VOl. 20, No. 6, 659-670, (1984)

15. W.F. Krupke, M.D. Shinn, J.E. Marion, J.A. Caird, and S.E. Stokowski, "Spectroscopic, optical, and thermomechanical properties of neodymium- and chromium-doped gadolinium scandium gallium garnet" J. Opt. Soc. Am.B. Vol. 3, No.1, 102-114 (1986)

16. A. Rapaport, S. Zhao, G. Xiao, A. Howard, and M. Bass, " Temperature dependence of the 1.06 mm stimulated emission cross section of neodymium in YAG and GSGG" Applied Optics Vol. 41, No. 23 7052-7057 (2002)

17. Y. Kalisky, "Cr^{4+}-doped crystals: their use as lasers and passive Q-switches", Progress in Quantum Electronics 28, 249–303, (2004)

18. H.Ridderbusch and T.Graf, "Saturation of 1047- and 1064- nm Absorption in Cr^{+4}:YAG Crystals", IEEE. J.QE. Vol.43.No.2, 168-173 (2007)

19. H. Eliers, U. Homerich, S. M. Jacobsen, and W. M. Yen, "Spectroscopic properties of Cr^{4+}:$Lu_3Al_5O_{12}$," *Opt. Lett.*, vol. 18, pp.1928-1930, (1993).

20. K.I. Borodin, V.A. Zhitnyuk, A.G. Ohrimtchyuk, and A.V. Shestakov, "Y3AL5O12-CR^{4+} LASER ACTION AT 1.34-μm to 1.6-μm" Izvestiya of Soviet Academy of Sciences, Fizika, Vol. 54, pg. 1500 1990.

21. Z. Burshtein, P. Blau, Y. Kalisky, Y. Shimony, and M.R. Kokta, "Excited-State Absorption Studies of Cr^{4+} Ions in Several Garent Host Crystals" IEEE.QE. Vol. 34. No. 2 292-299 (1998)

22. Y.Shimony, Z.Burshtein, and Y Kalisky, Cr^{+4}:YAG as a Passive Q-switch and Brewster Plate in a Pulsed Nd:YAG Laser", IEEE.J.QE. Vol.31, No.10 1738-1741, (1995)

23. G.Xiao, M.Bass, "Additional Experimental Confirmation of the Predictions of a model to Optimize Passively Q-switched Lasers" IEEE.J.QE. Vol. 34. No. 7 1143-1143, (1998)

24. L.Lin, B.Ouyang, and Y.Leng, "Mode-locking of Nd:YAG laser using Cr^{+4}:YAG crystal at 1.064μm" CLEO, CTuK36, Optical Society of America, Baltimore, MD, pg. 134 (1999)

25. A. Penzkofer, "Passive Q-switching nad Mode-Locking for the Generation of Nanosecond to Femtosecond Pulsed, " Appl. Phys. B. Vol. 46, pg. 43-60 (1988)

26. M.F. Becker, D.J. Kuizenga, A.E. Siegman, "Harmonic Mode Locking of Nd:YAG Laser" IEEE J.QE. Vol.8, 687-693 (1972)

27. J. Zabkar, M. Marincek, and M. Zgonik, " Mode Competition during the pulse formation in passively Q-switched Nd:Yag lasers" IEEE. J. QE. Vol. 44, No. 4 312-318, (2008)

6. DISTRIBUTION

1. MS0350 Art Fisher Org. 1123
2. MS1139 Alvaro Cruz-Cabrera Org. 1535
3. MS1153 Erik Zeek Org. 5444
4. MS1423 Michael Wanke Org. 1118
5. MS1423 Dave Bossert Org. 1118

1 MS0899 Technical Library 9536 (electronic copy)


Sandia National Laboratories